Electronic Supplementary Material (ESI) for Physical Chemistry Chemical Physics.

Electronic Supplementary Information

Infrared spectra of $HSCS^+$, *c*-HSCS, and HCS_2^- produced on electron-bombardment of CS_2 in solid *para*-hydrogen

Masashi Tsuge*[a] and Yuan-Pern Lee*[ab]

[a]*Department of Applied Chemistry and Institute of Molecular Sciences, National Chiao Tung University, 1001 Ta-Hsueh Road, Hsinchu 30010, Taiwan, E-mail: (MT) tsuge@nctu.edu.tw (YPL) yplee@mail.nctu.edu.tw, Tel: +886-3-5131459*

[b] *Institute of Molecular Sciences, Academia Sinica, Taipei 10617, Taiwan*

Electron bombardment of $^{13}CS_2$/p-H_2 matrices

The line of $^{13}CS_2^-$ was observed at 1123.3 cm^{-1}, consistent with the value 1122.2 cm^{-1} reported for $^{13}CS_2^-$ in a Ne matrix (Table S7).[1] The line of ^{13}CS was observed at 1236.6 cm^{-1}, consistent with values reported for ^{13}CS in *p*-H_2 (1236.4 cm^{-1})[2] and Ar (1239.5 cm^{-1}) matrices.[3] A line observed at 2160.0 cm^{-1} is tentatively assigned to $H^{13}C(S)SH^-$.

Lines of *t*-$HS^{13}CS$ were observed at 2530.5, 1251.8, 1202.9, 940.4, and 622.9 cm^{-1}, consistent with values 2527.5, 1247.1, 1201.0, 938.9, and 618.3 cm^{-1} reported for *t*-$HS^{13}CS$ in an Ar matrix;[4] Lines of *c*-$HS^{13}CS$ were observed at 2312.2 and 875.5 cm^{-1} (Table S4).

Weak lines of *t*-$H^{13}C(S)SH$ were observed at 1276.0, 1035.9, 926.4, 820.1, and 673.9 cm^{-1}, consistent with values 1280, 1037.5, 925.1, and 828 cm^{-1} reported for *t*-$H^{13}C(S)SH$ in an Ar matrix.[4] Lines of *c*-$H^{13}C(S)SH$ were observed at 1061.4 and 919.6 cm^{-1}, consistent with values 1062.7 and 918.2 cm^{-1} reported for *c*-$H^{13}C(S)SH$ in an Ar matrix;[4] the line of ν_3 is likely overlapped with the intense line at 1251.8 cm^{-1} of *t*-$HS^{13}CS$; the line of ν_6 corresponding to one observed in an Ar matrix at 799.0 cm^{-1} was unobserved because of its small intensity. These lines are listed in Table S6.

Electron bombardment of $C^{34}S_2$/p-H_2 matrices

The line of $C^{34}S_2^-$ was observed at 1157.4 cm^{-1}, consistent with the value 1153.5 cm^{-1} reported for $C^{34}S_2^-$ in a Ne matrix (Table S7).[1] The line of $C^{34}S$ was observed at 1262.5 cm^{-1}, consistent with values reported for $C^{34}S$ in *p*-H_2 (1262.1 cm^{-1})[2] and Ar (1264.9 cm^{-1}) matrices.[3] A line observed at 2159.0

cm^{-1}, with which an intense line of $C^{34}S_2$ ($\nu_1 + \nu_3$) interfered, is tentatively assigned to $HC(^{34}S)^{34}SH^-$.

Lines of *t*-$H^{34}SC^{34}S$ were observed at 2527.7, 1265.5, 1216.4, 940.7, and 621.6 cm^{-1}, consistent with values 2527.7, 1264.1, 1211.2, 939.2, and 617.1 cm^{-1} reported for *t*-$H^{34}SC^{34}S$ in an Ar matrix;[4] lines of *c*-$H^{34}SC^{34}S$ were observed at 2310.8 and 883.9 cm^{-1} (Table S4).

Weak lines of *t*-$HC(^{34}S)^{34}SH$ were observed at 1285.9, 1050.0, 933.7, 828.1, and 676.6 cm^{-1}, consistent with values 1289.1, 1052.1, 932.5, 835, and 674.8 cm^{-1} reported for *t*-$HC(^{34}S)^{34}SH$ in an Ar matrix.[4] Lines of *c*-$HC(^{34}S)^{34}SH$ were observed at 1074.6 and 922.2 cm^{-1}; the latter is tentatively assigned because of overlap. Observed wavenumbers are consistent with values 1076.4 and 921.4 cm^{-1} reported for *c*-$HC(^{34}S)^{34}SH$ in an Ar matrix.[4] The ν_3 mode of *c*-$HC(^{34}S)^{34}SH$ is unidentified because of interference from $C^{34}S$. These lines are listed in Table S6.

Discussion on [H_2, C, S_2] isomers, $HC(S)SH^-$, and CS_2^-

[H_2, C, S_2] isomers. The IR absorption lines of *t*-HC(S)SH at 1287.3, 1056.9, 934.6, 828.5, and 685.3 cm^{-1} in a CS_2/*p*-H_2 matrix and *c*-HC(S)SH at 1262.4, 1080.1, and 926.5 cm^{-1}, with those of their ^{13}C- and ^{34}S-isotopic variants, were confidently assigned on comparison with those reported for these species in an Ar matrix[4] and the predicted spectra and isotopic ratios, as listed in Table S6. The D-isotopic variants of these species were unidentified in the CS_2/*n*-D_2 experiment because D atoms have limited mobility in solid *n*-D_2.

Dithiohydroxy carbene HSCSH, another stable isomer of [H_2, C, S_2], has been studied both computationally and experimentally with a neutralization–reionization mass spectrometer.[5,6] According to the QCISD(T)/6-311++G(d,p) calculations by Nguyen *et al.*, the formation of HSCSH from HSCS + H is barrierless and exothermic by 200 kJ mol^{-1}, but the energy of HSCSH is greater than its acid isomers *t*-HC(S)SH and *c*-HC(S)SH by 160 kJ mol^{-1}. Furthermore, the energy of the transition state for the carbene–acid isomerization HSCSH → HC(S)SH is smaller than for HSCS + H by 73 kJ mol^{-1}, indicating that a reaction HSCS + H might result in the formation of acids *t*-HC(S)SH and *c*-HC(S)SH in solid *p*-H_2. The geometry of HSCSH was optimized; we calculated the harmonic and anharmonic IR spectra at the B3LYP/aug-cc-pVTZ level, as listed in Table S11. Anharmonic vibrational wavenumbers with IR intensities greater than 20 km mol^{-1} follow: 2160 (SH stretch, ν_7), 2145 (SH stretch, ν_1), 1020 (SCS antisymmetric stretch, ν_8), and 944 cm^{-1} (SH bend, ν_2). Among these modes, ν_1 and ν_8 have significant IR intensities, 165 and 91 km mol^{-1}, respectively, indicating that one might expect to observe a pair of lines, which show correlated variations at each step of the experiment, in the regions near 2150 and 1020 cm^{-1}. Although some lines are unassigned in these regions, none showed correlated variations; we hence exclude the possibility that HSCSH was produced in the present experiments.

$HC(S)SH^-$. The line observed at 2161.0 cm^{-1} in a CS_2/*p*-H_2 matrix is tentatively assigned to the SH-

stretching (ν_2) mode of HC(S)SH$^-$. The corresponding lines were observed at 2160.0 and 2159.0 cm^{-1} in $^{13}CS_2$/*p*-H_2 and $C^{34}S_2$/*p*-H_2 experiments, respectively. The observed wavenumber of the line near 2160 cm^{-1} and negligible isotopic shifts upon ^{13}C- and ^{34}S-substitution indicate that the absorption originates from an SH-stretching mode. The corresponding absorption around 2160 cm^{-1} was unidentified in a CS_2/*n*-D_2 matrix (see Fig. 6), confirming its assignment as an SH-stretching mode. We compared the observed line position (2161 cm^{-1}) with predicted spectra of SH$^-$ (2495 cm^{-1}, 79 km mol^{-1}), SH$^-$···CS complex (2411 cm^{-1}, 41 km mol^{-1}), *t*-HSCS$^-$ (2439 cm^{-1}, 40 km mol^{-1}), *c*-HSCS$^-$ (1969 cm^{-1}, 355 km mol^{-1}), HSC$^+$ (2157 cm^{-1}, 184 km mol^{-1}), HSCH$^+$ (3062 cm^{-1}, 106 km mol^{-1}), and HC(S)SH$^-$ (2144 cm^{-1}, 540 km mol^{-1}), of which predicted anharmonic wavenumbers and IR intensities of SH-stretching modes are shown in parentheses. The predicted anharmonic wavenumber of the SH-stretching mode of HSC$^+$ (2157 cm^{-1}) agrees with the observed wavenumber (2161.0 cm^{-1}); however, the SH-stretching mode of HSC$^+$ might be significantly red-shifted in solid *p*-H_2 due to proton sharing with *p*-H_2 host and, furthermore, the line of the CS-stretching mode is predicted to have a considerable IR intensity (1076 cm^{-1}, 133 km mol^{-1}) but features showing correlated changes with the 2161.0 cm^{-1} line were unobserved. Hence, we excluded the possibility that HCS$^+$ was produced in the present experiment. We found that only the predicted spectrum of HC(S)SH$^-$ matches with observation; the predicted anharmonic wavenumber of the SH-stretching (ν_2) mode agrees with the observed wavenumber and IR intensities of other modes are only a tenth or less, as listed in Table S10. The observation of only one line is thus consistent with the predictions, but observation of other lines is required to provide a definitive assignment.

CS_2^-. Although only one line (ν_3 at 1163.0 cm^{-1} in a CS_2/*p*-H_2 matrix) was observed, this line was confidently assigned to CS_2^- according to the expected chemistry, the agreement with values reported for CS_2^- in Ar and Ne matrices,[1,7] and a comparison of observed and quantum-chemically predicted ^{13}C- and ^{34}S-isotopic ratios; values are summarized in Table S7. In the electron-bombarded CS_2/*p*-H_2 matrix (Fig. 3), the mixing ratio of CS_2^- after deposition for 7 h was estimated to be 0.67 ppm; the mixing ratio decreased during maintenance of the matrix in darkness (−0.12 ppm) and during irradiation at 373 nm (−0.42 ppm). These decreases can be related to the production of HCS_2^-, as discussed previously. An increase (+0.11 ppm) was observed after irradiation at 254 nm, which might be due to photolysis of HCS_2^-. The yield of CS_2^- was significant (2.7 ppm) in the electron-bombarded CS_2/*n*-D_2 matrix (Fig. 6), because more electrons were trapped in solid *n*-D_2, but we are unable to identify the ν_1 line with a predicted anharmonic wavenumber at 618 cm^{-1} and IR intensity of 21 km mol^{-1}; the IR intensity of the ν_1 line is much smaller than that (561 km mol^{-1}) of the most intense ν_3 line.

References

1 M. Zhou and L. Andrews, *J. Chem. Phys.*, 2000, **112**, 6576-6582.

2 C.-W. Huang, Y.-C. Lee and Y.-P. Lee, *J. Chem. Phys.*, 2010, **132**, 164303.

3 R. B. Bohn, Y. Hannachi and L. Andrews, *J. Am. Chem. Soc.*, 1992, **114**, 6452-6459.

4 R. B. Bohn, G. D. Brabson and L. Andrews, *J. Phys. Chem.*, 1992, **96**, 1582-1589.

5 M. T. Nguyen, T. L. Nguyen and H. T. Le, *J. Phys. Chem. A*, 1999, **103**, 5758-5765.

6 S. Vivekananda, R. Srinivas, M. Manoharan and E. D. Jemmis, *J. Phys. Chem. A*, 1999, **103**, 5123-5128.

7 T. M. Halasinski, J. T. Godbout, J. Allison and G. E. Leroi, *J. Phys. Chem.*, 1996, **100**, 14865-14871.

Tables and Figures in the ESI

Vibrational wavenumbers and IR intensities predicted for $HSCS^+$, H_2–$HSCS^+$, HCS_2^+, and H_2–HCS_2^+ are compared in Table S1. Vibrational wavenumbers and IR intensities of $HSCS^+$, HCS_2^+, and their ^{13}C-, ^{34}S-, and D-isotopic variants are shown in Table S2; those of H_2–$HSCS^+$ and H_2–HCS_2^+ complexes and their isotopic variants are shown in Table S3. Vibrational wavenumbers and IR intensities of *t*-HSCS, *c*-HSCS, and HCS_2 isomers and their ^{13}C-, ^{34}S-, and D-isotopic variants are shown in Table S4. Relative energies of minima and transition states in the potential energy diagram of the H + CS_2 system are shown in Table S5. Vibrational wavenumbers and IR intensities of *t*-HC(S)SH, *c*-HC(S)SH, and their ^{13}C-, ^{34}S-, and D-isotopic variants are shown in Table S6. Vibrational wavenumbers and IR intensities of CS_2^-, $^{13}CS_2^-$, and $C^{34}S_2^-$ are shown in Table S7. Vibrational wavenumbers and IR intensities of HCS_2^-, $H^{13}CS_2^-$, $HC^{34}S_2^-$, and DCS_2^- are shown in Table S8. Vibrational wavenumbers and IR intensities of *t*-$HSCS^-$, *c*-$HSCS^-$, and their ^{13}C-, ^{34}S-, and D-isotopic variants are shown in Table S9. Vibrational wavenumbers and IR intensities of $HC(S)SH^-$ and its ^{13}C-, ^{34}S-, and D-isotopic variants are shown in Table S10. Vibrational wavenumbers and IR intensities of HSCSH are shown in Table S11.

Geometries of *t*-HSCS, *c*-HSCS, and HCS_2 are shown in Fig. S1. Potential energy diagram of the H + HSCS reaction is shown in FIG. S2. Geometries of HCS_2^-, *t*-$HSCS^-$, and *c*-$HSCS^-$ are shown in Fig. S3. Potential energy diagram of the H + CS_2^- is shown in Fig. S4. Partial infrared spectra of experiments with electron bombardment of CS_2/*p*-H_2 in the region 3300–2600 cm^{-1} are shown in Fig. S5. The observed spectrum is compared with spectra predicted for *t*-HSCS, *c*-HSCS, and HCS_2 in Fig. S6.

Table S1 Comparison of vibrational wavenumbers (in cm^{-1}) and IR intensities of $HSCS^+$, H_2–$HSCS^+$, HCS_2^+, and H_2–HCS_2^+ between experiments and quantum-chemical calculations

			Experiment	B3LYP/aug-cc-pVTZ		CCSD(T)/aug-cc-pVTZ	CCSD(T)/cc-pwVQZ[a]	
Molecule	Mode (sym.)[b]	Description	*p*-H_2	Harmonic	Anharmonic	Harmonic	Harmonic	Anharmonic
$HSCS^+$	ν_1 (A')	SH stretch	2477.2 (31)[c]	2573 (82)[d]	2424 (81)[d]	2610	2627 (553)[e]	2517
	ν_2 (A')	SCS asym stretch	1525.6 (100)	1562 (290)	1541 (257)	1535	1558 (342)	1537
	ν_3 (A')	HSC bend	919.6 (2)	935 (16)	913 (15)	938	945 (756)	924
	ν_4 (A')	SCS sym stretch		611 (2.7)	593 (2.4)	596	609 (43)	577
	ν_5 (A')	ip bend		322 (4.8)	328 (5.0)	307	316 (65)	320
	ν_6 (A'')	oop bend		374 (5.9)	381 (6.0)	361	372 (4)	377
H_2–$HSCS^+$	ν_1 (A')	SH stretch		2458 (418)	2330 (296)			
	ν_2 (A')	SCS asym stretch		1560 (327)	1535 (229)			
	ν_3 (A')	HSC bend		955 (22)	916 (26)			
	ν_4 (A')	SCS sym stretch		614 (3.4)	599 (3.0)			
	ν_5 (A')	ip bend		333 (4.2)	326 (4.3)			
	ν_6 (A'')	oop bend		375 (7.1)	369 (5.3)			
HCS_2^+	ν_1 (A_1)	CH stretch		3199 (70)	3058 (68)	3217		
	ν_2 (A_1)	SCS sym stretch		1050 (9.3)	1031 (9.6)	1039		
	ν_3 (A_1)	SCS bend		420 (0.8)	416 (0.9)	389		
	ν_4 (B_1)	oop CH bend		857 (26)	849 (26)	838		
	ν_5 (B_2)	HCS bend		1088 (0.1)	1068 (0.0)	1079		
	ν_6 (B_2)	SCS asym stretch		759 (93)	740 (92)	759		
H_2–HCS_2^+	ν_1 (A_1)	CH stretch		3157 (193)	3026 (146)			
	ν_2 (A_1)	SCS sym stretch		1048 (18)	1028 (15)			
	ν_3 (A_1)	SCS bend		421 (1.8)	416 (1.8)			
	ν_4 (B_1)	oop CH bend		886 (19)	840 (25)			
	ν_5 (B_2)	HCS bend		1103 (0.3)	1076 (0.1)			
	ν_6 (B_2)	SCS asym stretch		759 (88)	739 (85)			

[a] B. J. McIntosh, N. G. Adams and D. Smith, *Chem. Phys. Lett.* 1988, **148**, 142–148. [b] Mode numbers of H_2-$HSCS^+$ and H_2-HCS_2^+ follow those of $HSCS^+$ and HCS_2^+, respectively. Complete lists for H_2–$HSCS^+$ and H_2–HCS_2^+ are found in Table S3. [c] Relative integrated intensities are shown in parentheses. [d] Infrared intensities (in km mol^{-1}) are shown in parentheses. [e] Infrared intensities (in km mol^{-1}) calculated with the CCSD(T)(fc)/cc-pVTZ method are shown in parentheses.

Table S2 Vibrational wavenumbers (in cm^{-1}) and IR intensities of $HSCS^+$, HCS_2^+, and their ^{13}C-, ^{34}S-, and D-isotopic variants

			Experiment	B3LYP/aug-cc-pVTZ		CCSD(T)/cc-pwVQZ[a]	
Molecule	Mode (sym.)	Description	*p*-H_2	Harmonic	Anharmonic	Harmonic	Anharmonic
$HSCS^+$	ν_1 (A')	SH stretch	2477.2 (31)[b]	2573 (82)[c]	2424 (81)[c]	2627 (553)[d]	2517
	ν_2 (A')	SCS asym stretch	1525.6 (100)	1562 (290)	1541 (257)	1558 (342)	1537
	ν_3 (A')	HSC bend	919.6 (2)	935 (16)	913 (15)	945 (756)	924
	ν_4 (A')	SCS sym stretch		611 (2.7)	593 (2.4)	609 (43)	577
	ν_5 (A')	ip bend		322 (4.8)	328 (5.0)	316 (65)	320
	ν_6 (A'')	oop bend		374 (5.9)	381 (6.0)	372 (4)	377
$HS^{13}CS^+$	ν_1 (A')	SH stretch	2476.9 (37)	2572 (82)	2424 (82)		
	ν_2 (A')	$S^{13}CS$ asym stretch	1476.1 (100)	1512 (267)	1489 (251)		
	ν_3 (A')	$HS^{13}C$ bend	915.2 (3)	931 (16)	911 (13)		
	ν_4 (A')	$S^{13}CS$ sym stretch		611 (2.8)	591 (2.4)		
	ν_5 (A')	ip bend		312 (4.7)	320 (4.9)		
	ν_6 (A'')	oop bend		362 (6.2)	369 (6.3)		
$H^{34}SC^{34}S^+$	ν_1 (A')	^{34}SH stretch	2475.0 (38)	2570 (82)	2422 (82)		
	ν_2 (A')	$^{34}SC^{34}S$ asym stretch	1517.5 (100)	1554 (290)	1531 (271)		
	ν_3 (A')	$H^{34}SC$ bend	918.4 (2)	933 (16)	913 (15)		
	ν_4 (A')	$^{34}SC^{34}S$ sym stretch		594 (2.5)	578 (2.2)		
	ν_5 (A')	ip bend		320 (4.6)	327 (4.8)		
	ν_6 (A'')	oop bend		372 (5.6)	379 (5.7)		
$DSCS^+$	ν_1 (A')	SD stretch	1802.0 (20)	1848 (33)	1772 (32)		
	ν_2 (A')	SCS asym stretch	1524.4 (100)	1561 (296)	1538 (285)		
	ν_3 (A')	DSC bend	711.9 (4)	722 (11)	710 (9.5)		
	ν_4 (A')	SCS sym stretch		601 (2.7)	579 (2.3)		
	ν_5 (A')	ip bend		304 (3.4)	306 (3.5)		
	ν_6 (A'')	oop bend		372 (3.9)	375 (3.9)		
HCS_2^+	ν_1 (A_1)	CH stretch		3199 (70)	3058 (68)		
	ν_2 (A_1)	SCS sym stretch		1050 (9.3)	1031 (9.6)		
	ν_3 (A_1)	SCS bend		420 (0.8)	416 (0.9)		
	ν_4 (B_1)	oop CH bend		857 (26)	849 (26)		
	ν_5 (B_2)	HCS bend		1088 (0.1)	1068 (0.0)		
	ν_6 (B_2)	SCS asym stretch		759 (93)	740 (92)		
$H^{13}CS_2^+$	ν_1 (A_1)	^{13}CH stretch		3188 (71)	3047 (69)		
	ν_2 (A_1)	$S^{13}CS$ sym stretch		1023 (8.1)	1005 (8.4)		
	ν_3 (A_1)	$S^{13}CS$ bend		418 (0.7)	414 (0.8)		
	ν_4 (B_1)	oop ^{13}CH bend		849 (27)	842 (27)		
	ν_5 (B_2)	$H^{13}CS$ bend		1077 (0.1)	1059 (0.4)		
	ν_6 (B_2)	$S^{13}CS$ asym stretch		745 (88)	726 (87)		
$HC^{34}S_2^+$	ν_1 (A_1)	CH stretch		3199 (70)	3057 (68)		
	ν_2 (A_1)	$^{34}SC^{34}S$ sym stretch		1042 (9.7)	1023 (10)		
	ν_3 (A_1)	$^{34}SC^{34}S$ bend		409 (0.8)	405 (0.9)		
	ν_4 (B_1)	oop CH bend		856 (26)	849 (26)		
	ν_5 (B_2)	$HC^{34}S$ bend		1087 (0.0)	1068 (0.0)		
	ν_6 (B_2)	$^{34}SC^{34}S$ asym stretch		752 (93)	733 (92)		
DCS_2^+	ν_1 (A_1)	CD stretch		2374 (27)	2300 (27)		
	ν_2 (A_1)	SCS sym stretch		1012 (9.2)	994 (9.5)		
	ν_3 (A_1)	SCS bend		418 (0.8)	414 (0.8)		
	ν_4 (B_1)	oop CD bend		674 (9.4)	669 (9.6)		
	ν_5 (B_2)	DCS bend		913 (32)	892 (29)		
	ν_6 (B_2)	SCS asym stretch		657 (49)	646 (51)		

[a] M. C. McCarthy, P. Thaddeus, J. J. Wilke and H. F. Schaefer III, *J. Chem. Phys.*, 2009, **130**, 234304. [b] Relative integrated intensities are shown in parentheses. [c] Infrared intensities (in km mol^{-1}) are shown in parentheses. [d] Infrared intensities (in km mol^{-1}) calculated with the CCSD(T)(fc)/cc-pVTZ method are shown in parentheses.

Table S3 Predicted vibrational wavenumbers (in cm^{-1}) and IR intensities of H_2–$HSCS^+$ and H_2–HCS_2^+ complexes and their ^{13}C-, ^{34}S-, and D-isotopic variants.

Molecule	Mode	B3LYP/aug-cc-pVTZ		Molecule	Mode	B3LYP/aug-cc-pVTZ	
		Harmonic	Anharmonic			Harmonic	Anharmonic
H_2–$HSCS^+$	ν_1	4350 (71)[a]	4138 (63)[a]	H_2–HCS_2^+	ν_1	4381 (28)[a]	4170 (26)[a]
	ν_2 (ν_1)[b]	2458 (418)	2330 (296)		ν_2 (ν_1)[b]	3157 (193)	3026 (146)
	ν_3 (ν_2)	1560 (327)	1535 (229)		ν_3 (ν_5)	1103 (0.3)	1076 (0.1)
	ν_4 (ν_3)	955 (22)	916 (25)		ν_4 (ν_2)	1048 (18)	1028 (15)
	ν_5 (ν_4)	614 (3.4)	599 (3.0)		ν_5 (ν_4)	886 (19)	842 (25)
	ν_6	436 (0.0)	270 (2.3)		ν_6 (ν_6)	759 (88)	739 (85)
	ν_7 (ν_6)	375 (7.1)	369 (5.3)		ν_7 (ν_3)	421 (1.8)	416 (1.8)
	ν_8 (ν_5)	333 (4.2)	326 (4.3)		ν_8	379 (2.5)	222 (0.0)
	ν_9	246 (16)	206 (18)		ν_9	190 (6.4)	104 (3.2)
	ν_{10}	232 (24)	131 (11)		ν_{10}	72 (3.4)	36 (2.9)
	ν_{11}	110 (0.0)	31*i* (0.0)		ν_{11}	59 (0.0)	220*i* (0.0)
	ν_{12}	65 (0.1)	49 (0.0)		ν_{12}	47 (0.2)	19 (0.2)
H_2–$HS^{13}CS^+$	ν_1	4350 (71)	4136 (64)	H_2–$H^{13}CS_2^+$	ν_1	4381 (28)	4170 (26)
	ν_2 (ν_1)	2457 (419)	2330 (199)		ν_2 (ν_1)	3145 (195)	3013 (148)
	ν_3 (ν_2)	1510 (301)	1488 (278)		ν_3 (ν_5)	1093 (0.0)	1066 (0.0)
	ν_4 (ν_3)	952 (22)	911 (28)		ν_4 (ν_2)	1021 (16)	1003 (13)
	ν_5 (ν_4)	614 (3.5)	594 (3.1)		ν_5 (ν_4)	879 (19)	835 (27)
	ν_6	436 (0.0)	284 (1.7)		ν_6 (ν_6)	744 (83)	725 (80)
	ν_7 (ν_6)	363 (7.7)	357 (6.1)		ν_7 (ν_3)	419 (1.7)	415 (1.7)
	ν_8 (ν_5)	323 (4.3)	316 (4.1)		ν_8	379 (2.6)	222 (0.0)
	ν_9	246 (16)	206 (18)		ν_9	190 (6.4)	103 (3.2)
	ν_{10}	232 (24)	130 (10)		ν_{10}	71 (2.9)	39 (2.8)
	ν_{11}	110 (0.0)	44*i* (0.0)		ν_{11}	59 (0.0)	213*i* (0.0)
	ν_{12}	65 (0.1)	49 (0.0)		ν_{12}	47 (0.2)	21 (0.2)
H_2–$H^{34}SC^{34}S^+$	ν_1	4350 (70)	4136 (64)	H_2–$HC^{34}S_2^+$	ν_1	4381 (26)	4170 (26)
	ν_2 (ν_1)	2455 (419)	2330 (294)		ν_2 (ν_1)	3157 (193)	3012 (142)
	ν_3 (ν_2)	1552 (327)	1529 (304)		ν_3 (ν_5)	1102 (0.3)	1080 (0.0)
	ν_4 (ν_3)	954 (22)	913 (28)		ν_4 (ν_2)	1040 (19)	1021 (17)
	ν_5 (ν_4)	597 (3.1)	578 (2.5)		ν_5 (ν_4)	886 (19)	861 (25)
	ν_6	436 (0.0)	266 (2.2)		ν_6 (ν_6)	752 (88)	731 (88)
	ν_7 (ν_6)	373 (6.8)	366 (5.2)		ν_7 (ν_3)	410 (1.7)	405 (2.0)
	ν_8 (ν_5)	331 (4.0)	324 (4.2)		ν_8	379 (2.5)	226 (0.0)
	ν_9	246 (16)	206 (18)		ν_9	190 (6.3)	107 (3.2)
	ν_{10}	232 (24)	130 (10)		ν_{10}	72 (3.5)	24 (2.2)
	ν_{11}	110 (0.0)	44*i* (0.0)		ν_{11}	59 (0.0)	172*i* (0.0)
	ν_{12}	65 (0.2)	49 (0.0)		ν_{12}	47 (0.2)	39 (0.4)
D_2–$DSCS^+$	ν_1	3077 (35)	2969 (32)	D_2–DCS_2^+	ν_1	3099 (14)	2990 (13)

ν_2 (ν_1)	1768 (172)	1705 (118)	ν_2 (ν_1)	2344 (81)	2276 (65)
ν_3 (ν_2)	1557 (352)	1534 (329)	ν_3 (ν_2)	1009 (19)	990 (17)
ν_4 (ν_3)	731 (16)	712 (15)	ν_4 (ν_5)	915 (33)	892 (30)
ν_5 (ν_4)	605 (3.2)	583 (2.5)	ν_5 (ν_4)	692 (6.9)	671 (8.1)
ν_6	374 (3.7)	369 (4.1)	ν_6 (ν_6)	664 (47)	650 (47)
ν_7 (ν_5)	316 (3.0)	306 (3.4)	ν_7 (ν_3)	419 (1.7)	415 (1.6)
ν_8 (ν_6)	307 (0.2)	227 (0.0)	ν_8	269 (0.8)	198 (0.1)
ν_9	176 (8.2)	157 (8.6)	ν_9	136 (4.8)	90 (3.1)
ν_{10}	168 (15)	116 (7.1)	ν_{10}	61 (3.5)	37 (3.0)
ν_{11}	78 (0.0)	39 (0.0)	ν_{11}	42 (0.0)	57 (0.0)
ν_{12}	50 (0.0)	30 (0.1)	ν_{12}	37 (0.7)	3 (0.1)

[a] Infrared intensities (in km mol^{-1}) are shown in parentheses. [b] Mode numbers of corresponding monomers are given in parentheses.

Table S4 Vibrational wavenumbers (in cm^{-1}) and IR intensities of *t*-HSCS, *c*-HSCS, and HCS_2 isomers and their ^{13}C-, ^{34}S-, and D-isotopic variants

			Experiments		B3LYP/aug-cc-pVTZ		Literature	Isotopic ratio[a]			
Molecule	Mode (sym.)	Description	*p*-H_2	Ar[b]	Harmonic	Anharmonic	Harmonic	*p*-H_2	Ar	Harm.	Anharm.
t-HSCS	ν_1 (A')	SH stretch	2530.2[c] (<1)[d]	2527.5	2616 (0.4)[e]	2441 (2.1)[e]	2857[f]				
	ν_2 (A')	C═S stretch	1278.3[g] (81)	1275.2[g]	1267 (178)	1263 (178)	1358				
	ν_3 (A')	HSC bend	943.1 (30)	941.4	956 (29)	921 (22)	1062				
	ν_4 (A')	S–C stretch	632.4 (12)	627.9	635 (9.8)	617 (9.7)	669				
	ν_5 (A')	SCS bend	···	···	265 (3.1)	256 (2.9)	302				
	ν_6 (A'')	SH torsion	···	412.9	426 (19)	439 (18)	407				
	$2\nu_4$ (A')	overtone	1231.3[g] (100)	1227.8[g]	···	1206 (0.1)	···				
t-HS^{13}CS	ν_1 (A')	SH stretch	2530.5[c] (<1)	2527.5	2616 (0.4)	2444 (2.1)	···	1.000	1.000	1.000	1.001
	ν_2 (A')	^{13}C═S stretch	1251.8[g] (53)	1247.1[g]	1229 (164)	1233 (163)	···	···	···	···	···
	ν_3 (A')	HS^{13}C bend	940.4 (32)	938.9	953 (30)	917 (23)	···	0.997	0.997	0.997	0.996
	ν_4 (A')	S–C stretch	622.9 (11)	618.3	625 (9.6)	608 (9.6)	···	0.985	0.985	0.984	0.985
	ν_5 (A')	S^{13}CS bend	···	···	260 (3.0)	251 (2.8)	···	···	···	0.983	0.980
	ν_6 (A'')	SH torsion	···	···	422 (19)	439 (18)	···	···	···	0.991	0.999
	$2\nu_4$ (A')	overtone	1202.9[g] (100)	1201.0[g]	···	1182 (0.1)	···	···	···	···	···
t-H^{34}SC^{34}S	ν_1 (A')	^{34}SH stretch	2527.7[c] (<1)	2527.7	2614 (0.4)	2442 (2.2)	···	···	1.000	0.999	1.000
	ν_2 (A')	C═^{34}S stretch	1265.5[g] (100)	1264.1[g]	1261 (177)	1252 (175)	···	···	···	···	···
	ν_3 (A')	H^{34}SC bend	940.7 (22)	939.2	953 (29)	918 (23)	···	0.998	0.998	0.997	0.997
	ν_4 (A')	^{34}S–C stretch	621.6 (7)	617.1	625 (9.5)	606 (9.3)	···	0.983	0.983	0.983	0.982
	ν_5 (A')	^{34}SC^{34}S bend	···	···	260 (2.9)	251 (2.8)	···	···	···	0.984	0.982
	ν_6 (A'')	^{34}SH torsion	···	412.8	425 (19)	441 (18)	···	···	1.000	0.999	1.004
	$2\nu_4$ (A')	overtone	1216.4[g] (44)	1211.2[g]	···	1188 (0.1)	···	···	···	···	···
t-DSCS	ν_1 (A')	SD stretch	1827.7 (1)	1805.3	1880 (0.4)	1791 (3.7)	···	0.717	0.714	0.719	0.734
	ν_2 (A')	C═S stretch	1252.6[g] (100)	1249.7[g]	1252 (196)	1240 (186)	···	···	···	···	···
	ν_3 (A')	DSC bend	716.6 (17)	713.8	721 (17)	708 (16)	···	0.760	0.758	0.754	0.767
	ν_4 (A')	S–C stretch	618.8 (3)	614.8	622 (4.2)	607 (3.9)	···	0.979	0.979	0.978	0.984
	ν_5 (A')	SCS bend	···	···	260 (2.8)	254 (2.7)	···	···	···	0.985	0.992
	ν_6 (A'')	SD torsion	···	···	340 (10)	340 (10)	···	···	···	0.985	0.992
	$2\nu_4$ (A')	overtone	1218.7[g] (73)	1213.1[g]	···	1195 (0.0)	···	···	···	···	···
c-HSCS	ν_1 (A')	SH stretch	2312.7 (73)	···	2433 (47)	2255 (72)	2834[f]				
	ν_2 (A')	C═S stretch	OVL[h]	···	1286 (168)	1273 (150)	1355				
	ν_3 (A')	HSC bend	889.0 (100)	···	938 (48)	918 (43)	1052				
	ν_4 (A')	S–C stretch	···	···	599 (2.7)	586 (2.8)	633				
	ν_5 (A')	SCS bend	···	···	243 (5.8)	235 (5.9)	303				
	ν_6 (A'')	SH torsion	···	···	437 (1.4)	429 (1.3)	413				
c-HS^{13}CS	ν_1 (A')	SH stretch	2312.2 (82)	···	2433 (46)	2255 (72)	···	1.000	···	1.000	1.000
	ν_2 (A')	^{13}C═S stretch	OVL[h]	···	1245 (157)	1234 (153)	···	···	···	0.968	0.970
	ν_3 (A')	HS^{13}C bend	875.5 (100)	···	934 (47)	914 (43)	···	0.985	···	0.996	0.996

	ν_4 (A')	S–C stretch	···	···	594 (2.6)	581 (2.8)	···	···	···	0.991	0.992
	ν_5 (A')	S^{13}CS bend	···	···	238 (5.6)	230 (5.7)	···	···	···	0.979	0.977
	ν_6 (A'')	SH torsion	···	···	431 (1.6)	424 (1.2)	···	···	···	0.987	0.988
c-H^{34}SC^{34}S	ν_1 (A')	^{34}SH stretch	2310.8 (100)	···	2431 (47)	2253 (72)	···	0.999	···	0.999	0.999
	ν_2 (A')	C═^{34}S stretch	OVL[h]	···	1279 (166)	1265 (151)	···	···	···	0.994	0.994
	ν_3 (A')	H^{34}SC bend	883.9 (70)	···	937 (47)	918 (43)	···	0.994	···	0.999	0.999
	ν_4 (A')	^{34}S–C stretch	···	···	585 (2.7)	573 (2.8)	···	···	···	0.977	0.977
	ν_5 (A')	^{34}SC^{34}S bend	···	···	240 (5.6)	232 (5.8)	···	···	···	0.989	0.989
	ν_6 (A'')	^{34}SH torsion	···	···	436 (1.4)	429 (1.3)	···	···	···	0.996	0.998
c-DSCS	ν_1 (A')	SD stretch	···	···	1748 (27)	1657 (36)	···	···	···	0.718	0.735
	ν_2 (A')	C═S stretch	···	···	1286 (165)	1263 (126)	···	···	···	1.000	0.992
	ν_3 (A')	DSC bend	···	···	718 (37)	701 (33)	···	···	···	0.765	0.763
	ν_4 (A')	S–C stretch	···	···	593 (0.9)	581 (1.1)	···	···	···	0.989	0.991
	ν_5 (A')	SCS bend	···	···	229 (4.4)	224(4.5)	···	···	···	0.944	0.954
	ν_6 (A'')	SD torsion	···	···	375 (0.0)	370 (0.0)	···	···	···	0.859	0.863
HCS_2	ν_1 (A_1)	CH stretch	···	···	3129 (3.6)	2976 (7.8)	3170 [i]				
	ν_2 (A_1)	CS_2 sym stretch	···	···	901 (1.9)	887 (2.1)	914				
	ν_3 (A_1)	CS_2 bend	···	···	307 (0.1)	302 (0.2)	311				
	ν_4 (B_1)	oop CH bend	···	···	830 (24)	823 (22)	2286				
	ν_5 (B_2)	ip CH bend	···	1252.9[c]	1219 (10)	1209 (14)	2995				
	ν_6 (B_2)	CS_2 asym stretch	···	1004.9[c]	902 (44)	883 (39)	1112				
$H^{13}CS_2$	ν_1 (A_1)	^{13}CH stretch	···	···	3119 (3.5)	2966 (7.6)	···	···	···	0.997	0.997
	ν_2 (A_1)	$^{13}CS_2$ sym stretch	···	···	880 (1.7)	866 (2.0)	···	···	···	0.976	0.977
	ν_3 (A_1)	$^{13}CS_2$ bend	···	···	305 (0.1)	300 (0.2)	···	···	···	0.994	0.995
	ν_4 (B_1)	oop ^{13}CH bend	···	···	822 (24)	814 (23)	···	···	···	0.989	0.989
	ν_5 (B_2)	ip ^{13}CH bend	···	1252.3[c]	1212 (12)	1200 (16)	···	···	1.000	0.994	0.992
	ν_6 (B_2)	$^{13}CS_2$ asym stretch	···	977.9[c]	879 (40)	861 (36)	···	···	0.973	0.975	0.975
$HC^{34}S_2$	ν_1 (A_1)	CH stretch	···	···	3129 (3.6)	2975 (7.8)	···	···	···	1.000	1.000
	ν_2 (A_1)	$C^{34}S_2$ sym stretch	···	···	892 (1.8)	878 (2.1)	···	···	···	0.990	0.990
	ν_3 (A_1)	$C^{34}S_2$ bend	···	···	299 (0.1)	295 (0.2)	···	···	···	0.975	0.976
	ν_4 (B_1)	oop CH bend	···	···	831 (24)	823 (23)	···	···	···	1.000	0.999
	ν_5 (B_2)	ip CH bend	···	···	1220 (10)	1207 (14)	···	···	···	1.000	0.998
	ν_6 (B_2)	$C^{34}S_2$ asym stretch	···	999.0[c]	895 (43)	877 (39)	···	···	0.994	0.993	0.993
DCS_2	ν_1 (A_1)	CD stretch	···	···	2307 (2.8)	2229 (4.7)	···	···	···	0.737	0.749
	ν_2 (A_1)	CS_2 sym stretch	···	···	876 (1.6)	863 (1.7)	···	···	···	0.972	0.973
	ν_3 (A_1)	CS_2 bend	···	···	305 (0.1)	301 (0.2)	···	···	···	0.994	0.995
	ν_4 (B_1)	oop CD bend	···	···	669 (10)	664 (10)	···	···	···	0.806	0.806
	ν_5 (B_2)	ip CD bend	···	1065.5[c]	1008 (5.0)	985 (2.5)	···	···	0.850	0.826	0.815
	ν_6 (B_2)	CS_2 asym stretch	···	853.0[c]	786 (33)	776 (34)	···	···	0.849	0.872	0.880

[a] Isotopic ratio is defined as the ratio of wavenumber of the isotopic species to that of the naturally abundant species. [b] R. B. Bohn, G. D. Brabson and L. Andrews, *J. Phys. Chem.*, 1992, **96**, 1582–1589. [c] Tentative assignment. [d] Relative infrared intensities are shown in

parentheses. [e] Infrared intensities (in km mol^{-1}) are shown in parentheses. [f] Harmonic vibrational wavenumbers calculated at the DZP level using the HONDO 7.0 program; R. B. Bohn, G. D. Brabson and L. Andrews, *J. Phys. Chem.*, 1992, **96**, 1582–1589. [g] Fermi resonance. [h] Unidentified preferably due to interference from the intense line of corresponding *t*-HSCS isotopic variants. [i] Harmonic vibrational wavenumbers calculated with the mPW2PLYP/aug-cc-pVTZ method; Z. Qin, R. Cong, Z. Liu, H. Xie, Z. Tang, and H. Fan, *J. Chem. Phys.*, 2014, **140**, 214318. Predicted wavenumbers for the ν_4 (2286 cm^{-1}) and ν_5 (2995 cm^{-1}) modes are abnormally high for the CH-bending modes most probably due to an inappropriate choice of method.

Table S5 Zero-point-energy corrected relative energies (in kJ mol^{-1}) of minima and transition states (TS) in the potential energy diagram of the H + CS_2 system calculated at the B3LYP and CCSD(T) levels with the aug-cc-pVTZ basis set

	Description	B3LYP	CCSD(T)
a	H + CS_2	0.0	0.0
b	HS + CS	92.8	76.1
c	HCS_2	−105.4	−98.5
d	*t*-HSCS	−67.5	−63.4
e	*c*-HSCS	−66.0	−60.2
f	TS: H + CS_2 → HCS_2	28.9	36.9
g	TS: H + CS_2 → *c*-HSCS	1.7	0.0
h	TS: HCS_2 → *t*-HSCS	46.6	51.9
i	TS: *c*-HSCS → *t*-HSCS (bending)	−52.6	−39.9
j	TS: *c*-HSCS → *t*-HSCS (torsional)	−3.6	−18.6

Table S6 Vibrational wavenumbers (in cm^{-1}) and IR intensities of *t*-HC(S)SH and *c*-HC(S)SH isomers and their ^{13}C-, ^{34}S- and D-isotopic variants

Molecule	Mode (sym.)	Description	Experiments			B3LYP/aug-cc-pVTZ		Literature	Isotopic ratio[a]			
			p-H_2	Ar[b]	Gas[c]	Harmonic	Anharmonic	Harmonic	p-H_2	Ar	Harm.	Anharm.
t-HC(S)SH	ν_1 (A')	CH stretch	···	···	2988.8	3094 (5.2)[d]	2947 (8.7)[d]	3343[e]				
	ν_2 (A')	SH stretch	···	···	···	2650 (1.2)	2482 (0.7)	2875				
	ν_3 (A')	HCS deform	1287.3 (40)[f]	1290.5	1283.0	1318 (56)	1288 (46)	1469				
	ν_4 (A')	C═S stretch	1056.9 (100)	1059.8	1057.2	1066 (139)	1052 (132)	1166				
	ν_5 (A')	CSH deform	934.6 (24)	933.4	935.5	941 (53)	923 (51)	1054				
	ν_6 (A')	C–S stretch	685.3 (30)	682.6	682.5	682 (42)	668 (44)	759				
	ν_7 (A')	S–C–SH bend	···	···	···	323 (2.6)	321 (2.3)	357				
	ν_8 (A'')	oop CH bend	828.5 (23)	836.8	824.0	850 (32)	832 (31)	951				
	ν_9 (A'')	SH torsion	···	···	···	440 (5.3)	398 (6.0)	449				
t-H^{13}C(S)SH	ν_1 (A')	^{13}CH stretch	···	···	···	3084 (5.1)	2938 (8.6)	···	···	···	0.997	0.997
	ν_2 (A')	SH stretch	···	···	···	2650 (1.2)	2482 (0.7)	···	···	···	1.000	1.000
	ν_3 (A')	H^{13}CS deform	1276.0 (28)	1280	···	1308 (42)	1278 (32)	···	0.991	0.992	0.992	0.992
	ν_4 (A')	^{13}C═S stretch	1035.9 (100)	1037.5	···	1044 (133)	1030 (128)	···	0.980	0.979	0.979	0.980
	ν_5 (A')	^{13}CSH deform	926.4 (52)	925.1	···	932 (56)	915 (53)	···	0.991	0.991	0.991	0.991
	ν_6 (A')	^{13}C–S stretch	673.9 (35)	···	···	670 (41)	656 (43)	···	0.983	···	0.983	0.983
	ν_7 (A')	S–^{13}C–SH bend	···	···	···	320 (2.6)	318 (2.3)	···	···	···	0.992	0.991
	ν_8 (A'')	oop ^{13}CH bend	820.1 (25)	828	···	841 (32)	824 (31)	···	0.990	0.990	0.990	0.990
	ν_9 (A'')	SH torsion				438 (5.1)	395 (5.7)	···	···	···	0.994	0.992
t-HC(^{34}S)^{34}SH	ν_1 (A')	CH stretch	···	···	···	3094 (5.2)	2947 (8.8)	···	···	···	1.000	1.000
	ν_2 (A')	^{34}SH stretch	···	···	···	2648 (1.2)	2480 (0.7)	···	···	···	0.999	0.999
	ν_3 (A')	HC^{34}S deform	1285.9 (32)	1289.1	···	1317 (55)	1286 (40)	···	0.999	0.999	1.000	0.998
	ν_4 (A')	C═^{34}S stretch	1050.0 (100)	1052.1	···	1059 (137)	1045 (130)	···	0.993	0.993	0.993	0.993
	ν_5 (A')	C^{34}SH deform	933.7 (26)	932.5	···	939 (55)	922 (53)	···	0.999	0.999	0.999	0.998
	ν_6 (A')	C–^{34}S stretch	676.6 (31)	674.8	···	674 (40)	659 (43)	···	0.987	0.989	0.988	0.988
	ν_7 (A')	^{34}S–C–^{34}SH bend	···	···	···	316 (2.4)	314 (2.1)	···	···	···	0.980	0.979
	ν_8 (A'')	oop CH bend	828.1 (25)	835	···	849 (32)	832 (31)	···	1.000	0.998	1.000	1.000
	ν_9 (A'')	^{34}SH torsion	···	···	···	439 (5.3)	396 (5.9)	···	···	···	0.998	0.996
t-DC(S)SD	ν_1 (A')	CD stretch	···	···	···	2277 (3.6)	2173 (4.8)	2642	···	···	0.736	0.737
	ν_2 (A')	SD stretch	···	···	···	1903 (0.5)	1817 (0.3)	2063	···	···	0.718	0.732
	ν_3 (A')[g]	DCS deform	···	867	···	879 (13)	867 (11)	958	0.672	0.731	0.666	0.673
	ν_4 (A')[g]	C═S stretch	···	1133.5	1150.5	1142 (207)	1120 (192)	1277	1.070	1.088	1.072	1.065
	ν_5 (A')	CSD deform	···	764.5	···	764 (45)	752 (42)	843	0.819	···	0.813	0.814
	ν_6 (A')	C–S stretch	···	622	660.5	619 (18)	610 (18)	765	0.911	0.968	0.908	0.914
	ν_7 (A')	S–C–SH bend	···	···	···	304 (2.7)	302 (2.5)	694	···	···	0.940	0.940

	ν_8 (A'')	oop CD bend	···	670	668.0	682 (16)	672 (15)	344	0.801	0.811	0.802	0.807
	ν_9 (A'')	SD torsion	···	···	···	339 (4.2)	317 (4.4)	337	···	···	0.770	0.796
c-HC(S)SH	ν_1 (A')	CH stretch	···	···	···	3101 (7.5)	2960 (12)	3352				
	ν_2 (A')	SH stretch	···	···	···	2648 (0.8)	2481 (1.8)	2862				
	ν_3 (A')	HCS deform	1262.4 (100)	1265.4	1255.5	1289 (84)	1262 (76)	1449				
	ν_4 (A')	C═S stretch	1080.1 (93)	1082.2	1080.8	1092 (98)	1075 (92)	1202				
	ν_5 (A')	CSH deform	926.5 (93)	922.5	···	933 (87)	918 (76)	1050				
	ν_6 (A')	C–S stretch	···	725.8	710.0	721 (29)	707 (36)	785				
	ν_7 (A')	S–C–SH bend	···	···	···	301 (0.1)	300 (0.1)	335				
	ν_8 (A'')	oop CH bend	···	807.2	794.5	817 (29)	805 (27)	915				
	ν_9 (A'')	SH torsion	···	···	···	381 (13)	350 (13)	365				
c-H^{13}C(S)SH	ν_1 (A')	^{13}CH stretch	···	···	···	3092 (7.3)	2951 (12)	···	···	···	0.997	0.997
	ν_2 (A')	SH stretch	···	···	···	2648 (0.8)	2481 (1.8)	···	···	···	1.000	1.000
	ν_3 (A')	H^{13}CS deform	OVL[h]	1255	···	1278 (63)	1251 (57)	···	···	0.992	0.992	0.992
	ν_4 (A')	^{13}C═S stretch	1061.4 (89)	1062.7	···	1073 (94)	1056 (89)	···	0.983	0.982	0.982	0.982
	ν_5 (A')	^{13}CSH deform	919.6 (100)	918.2	···	925 (91)	911 (80)	···	0.993	0.992	0.992	0.992
	ν_6 (A')	^{13}C–S stretch	···	···	···	706 (31)	692 (37)	···	···	···	0.979	0.979
	ν_7 (A')	S–^{13}C–SH bend	···	···	···	299 (0.1)	298 (0.1)	···	···	···	0.993	0.993
	ν_8 (A'')	oop ^{13}CH bend	···	799.0	···	807 (28)	796 (27)	···	···	0.990	0.988	0.988
	ν_9 (A'')	SH torsion	···	···	···	380 (14)	349 (13)	···	···	···	0.997	0.997
c-HC(^{34}S)^{34}SH	ν_1 (A')	CH stretch	···	···	···	3103 (7.5)	2960 (12)	···	···	···	1.000	1.000
	ν_2 (A')	^{34}SH stretch	···	···	···	2645 (0.8)	2479 (1.8)	···	···	···	0.999	0.999
	ν_3 (A')	HC^{34}S deform	OVL[i]	···	···	1288 (82)	1261 (74)	···	···	···	1.000	0.999
	ν_4 (A')	C═^{34}S stretch	1074.6 (63)	1076.4	···	1087 (96)	1070 (91)	···	0.995	0.995	0.995	0.995
	ν_5 (A')	C^{34}SH deform	922.2[j] (100)	921.4	···	928 (88)	913 (77)	···	0.995	0.996	0.995	0.995
	ν_6 (A')	C–^{34}S stretch	···	···	···	714 (29)	701 (35)	···	···	···	0.991	0.992
	ν_7 (A')	^{34}S–C–^{34}SH bend	···	···	···	294 (0.1)	293 (0.1)	···	···	···	0.977	0.976
	ν_8 (A'')	oop CH bend	···	806.1	···	816 (29)	805 (28)	···	···	0.999	0.999	0.999
	ν_9 (A'')	^{34}SH torsion	···	···	···	381 (13)	349 (13)	···	···	···	0.999	0.999
c-DC(S)SD	ν_1 (A')	CD stretch	···	···	···	2285 (5.3)	2175 (6.6)	2470	···	···	0.737	0.735
	ν_2 (A')	SD stretch	···	···	···	1901 (0.4)	1816 (0.6)	2055	···	···	0.718	0.732
	ν_3 (A')	DCS deform	···	1123.4	···	1132 (231)	1111 (216)	1271	···	0.888	0.879	0.881
	ν_4 (A')	C═S stretch	···	···	···	879 (1.1)	864 (1.1)	968	···	···	0.805	0.804
	ν_5 (A')	CSD deform	···	776.7	···	779 (55)	765 (55)	863	···	0.839	0.835	0.834
	ν_6 (A')	C–S stretch	···	613.3	···	622 (6.1)	613 (7.0)	687	···	0.845	0.863	0.868
	ν_7 (A')	S–C–SD bend	···	···	···	295 (0.1)	294 (0.1)	269	···	···	0.979	0.979
	ν_8 (A'')	oop CD bend	···	655.8	···	667 (15)	659 (15)	748	···	0.812	0.817	0.819
	ν_9 (A'')	SD torsion	···	···	···	281 (4.6)	265 (4.5)	329	···	···	0.736	0.757

[a] Isotopic ratio is defined as the ratio of wavenumber of the isotopic species to that of the naturally abundant species. [b] R. B. Bohn, G. D.

Brabson and L. Andrews, *J. Phys. Chem.*, 1992, **96**, 1582–1589. [c] F. Ioannoni, D. C. Moule, J. D. Goddard and D. J. Clouthier, *J. Mol. Struct*. 1989, **197**, 159–170. [d] Infrared intensities (in km mol^{-1}) are shown in parentheses. [e] Harmonic vibrational wavenumbers calculated at the DZP level using the HONDO 7.0 program; R. B. Bohn, G. D. Brabson and L. Andrews, *J. Phys. Chem.*, 1992, **96**, 1582–1589. [f] Relative infrared intensities are shown in parentheses. [g] Mode numbers follow those of *t*-HC(S)SH. These modes are mixed, resulting in anomalous isotopic ratios. [h] Unidentified probably due to interference from the intense 1251.8 cm^{-1} line of *t*-$HS^{13}CS$. [i] Unidentified probably due to interference from the 1265.7 cm^{-1} line of $^{12}C^{34}S$. [j] Tentative assignment.

Table S7 Vibrational wavenumbers (in cm^{-1}) and IR intensities of CS_2^-, $^{13}CS_2^-$, and $C^{34}S_2^-$

			Experiments			B3LYP/aug-cc-pVTZ		Isotopic ratio[a]				
Species	Mode (sym.)	Description	*p*-H_2	Ne[b,c]	Ar[c]	Harmonic	Anharmonic	*p*-H_2	Ne	Ar	Harmonic	Anharmonic
CS_2^-	ν_1 (A_1)	sym stretch	···	···	···	645 (23)	618 (21)					
	ν_2 (A_1)	bend	···	···	···	322 (10)	318 (9.4)					
	ν_3 (B_2)	asym stretch	1163.0	1159.2	1160.4	1174 (580)	1155 (561)					
$^{13}CS_2^-$	ν_1 (A_1)	sym stretch	···	···	···	636 (20)	641 (20)	···	···	···	0.986	1.037
	ν_2 (A_1)	bend	···	···	···	316 (9.3)	312 (8.9)	···	···	···	0.981	0.981
	ν_3 (B_2)	asym stretch	1123.3	1122.2	1123.3	1136 (547)	1118 (530)	0.966	0.968	0.968	0.968	0.968
$C^{34}S_2^-$	ν_1 (A_1)	sym stretch	···	···	···	633 (23)	608 (22)	···	···	···	0.981	0.983
	ν_2 (A_1)	bend	···	···	···	317 (9.7)	313 (9.3)	···	···	···	0.984	0.984
	ν_3 (B_2)	asym stretch	1157.4	1153.5	1154.8	1168 (570)	1149 (551)	0.995	0.995	0.995	0.995	0.995

[a] Isotopic ratio is defined as the ratio of wavenumber of the isotopic species to that of the naturally abundant species. [b] T. M. Halasinski, J. T. Godbout, J. Allison and G. E. Leroi, *J. Phys. Chem.*, 1996, **100**, 14865–14871. [c] M. Zhou and L. Andrews, *J. Chem. Phys*., 2000, **112**, 6576–6582.

Table S8 Vibrational wavenumbers (in cm^{-1}) and IR intensities of HCS_2^- and its ^{13}C-, ^{34}S- and D-isotopic variants

Molecule	Mode (sym.)	Description[c]	Experiment	B3LYP/aug-cc-pVTZ		mPW2PLYP[a]	Isotopic ratio[b]		
			p-H_2	Harmonic	Anharmonic	Harmonic	p-H_2	Harmonic	Anharmonic
HCS_2^-	ν_1 (A_1)	CH stretch	2875.7 (12)[d]	3011 (46)[e]	2841 (70)[e]	3049			
	ν_2 (A_1)	SCS sym stretch	···	772 (0.0)	760 (0.0)	781			
	ν_3 (A_1)	SCS bend	···	344 (0.5)	342 (0.5)	347			
	ν_4 (B_1)	oop CH bend	814.3[f] (43)	822 (36)	815 (34)	831			
	ν_5 (B_2)	HCS bend	1249.9 (9)	1269 (89)	1244 (79)	1277			
	ν_6 (B_2)	SCS asym stretch	1003.2 (100)	1002 (470)	983 (461)	1022			
$H^{13}CS_2^-$	ν_1 (A_1)	^{13}CH stretch	2867.0 (14)	3001 (47)	2832 (70)	···	0.997	0.997	0.997
	ν_2 (A_1)	S^{13}CS sym stretch	···	754 (0.0)	743 (0.0)	···	···	0.998	0.978
	ν_3 (A_1)	S^{13}CS bend	···	341 (0.4)	339 (0.4)	···	···	0.992	0.992
	ν_4 (B_1)	oop ^{13}CH bend	807.5[f] (7)	811 (36)	804 (33)	···	0.992	0.987	0.987
	ν_5 (B_2)	H^{13}CS bend	OVL[g]	1263 (67)	1239 (58)	···	···	0.995	0.996
	ν_6 (B_2)	S^{13}CS asym stretch	976.9 (100)	975 (461)	956 (452)	···	0.974	0.972	0.973
$HC^{34}S_2^-$	ν_1 (A_1)	CH stretch	2875.7 (13)	3011 (46)	2841 (70)	···	1.000	1.000	1.000
	ν_2 (A_1)	^{34}SC^{34}S sym stretch	···	763 (0.1)	751 (0.0)	···	···	0.989	0.989
	ν_3 (A_1)	^{34}SC^{34}S bend	···	336 (0.5)	333 (0.5)	···	···	0.976	0.977
	ν_4 (B_1)	oop CH bend	OVL[h]	822 (37)	814 (34)	···	···	0.999	0.999
	ν_5 (B_2)	HC^{34}S bend	1249.9 (9)	1268 (89)	1244 (78)	···	1.000	1.000	1.000
	ν_6 (B_2)	^{34}SC^{34}S asym stretch	1003.2 (100)	996 (461)	977 (452)	···	0.994	0.994	0.994
DCS_2^-	ν_1 (A_1)	CD stretch	2176.0 (4)	2214 (22)	2145 (70)	···	0.757	0.735	0.755
	ν_2 (A_1)	SCS sym stretch	···	753 (0.0)	743 (0.0)	···	···	0.976	0.978
	ν_3 (A_1)	SCS bend	···	341 (0.4)	339 (0.4)	···	···	0.992	0.992
	ν_4 (B_1)	oop CD bend	679.2 (4)	681 (20)	675 (19)	···	0.834	0.828	0.829
	ν_5 (B_2)[i]	DCS bend	852.2 (14)	860 (65)	848 (67)	···	0.682	0.678	0.681
	ν_6 (B_2)[i]	SCS asym stretch	1067.8 (100)	1062 (492)	1041 (474)	···	1.064	1.060	1.060

[a] With the aug-cc-pVTZ basis set; Z. Qin, R. Cong, Z. Liu, H. Xie Z. Tang and H. Fan, *J. Chem. Phys.*, 2014, **140**, 214318. [b] Isotopic ratio is defined as the ratio of wavenumber of the isotopic species to that of the naturally abundant species. [c] oop, out-of-plane. [d] Relative infrared intensities are shown in parentheses. [e] Infrared intensities (in km mol^{-1}) are shown in parentheses. [f] Tentative assignments. [g] Unidentified probably due to interference from the 1236.6 cm^{-1} line of ^{13}CS. [h] Unidentified due to interference from features of unassigned species around 810 cm^{-1}. [i] Mode numbers follow those of HCS_2^-.

Table S9 Vibrational wavenumbers (in cm^{-1}) and IR intensities of *t*-$HSCS^-$ and *c*-$HSCS^-$ isomers and their ^{13}C-, ^{34}S- and D-isotopic variants calculated with the B3LYP/aug-cc-pVTZ method

			[H, ^{12}C, ^{32}S]		[H, ^{13}C, ^{32}S]		[H, ^{12}C, ^{34}S]		[D, ^{12}C, ^{32}S]	
Isomer	Mode	Description	Harmonic	Anharmonic	Harmonic	Anharmonic	Harmonic	Anharmonic	Harmonic	Anharmonic
t-$HSCS^-$	ν_1 (*A′*)	SH stretch	2606 (25)[a]	2439 (40)[a]	2606 (25)[a]	2441 (39)[a]	2603 (25)[a]	2439 (39)[a]	1871 (12)[a]	1784 (18)[a]
	ν_2 (*A′*)	HSC bend + CS stretch	981 (139)	971 (178)	964 (112)	943 (149)	977 (134)	968 (172)	924 (240)	879 (231)
	ν_3 (*A′*)	HSC bend + CS stretch	814 (136)	783 (95)	809 (148)	777 (108)	813 (137)	778 (98)	646 (55)	616 (49)
	ν_4 (*A′*)	(H)SC stretch	517 (116)	478 (128)	501 (112)	464 (119)	514 (113)	476 (125)	507 (96)	470 (99)
	ν_5 (*A′*)	SCS bend	269 (10)	257 (13)	268 (10)	256 (12)	262 (10)	250 (12)	266 (10)	255 (12)
	ν_6 (*A″*)	SH torsion	430 (14)	453 (13)	429 (13)	454 (12)	430 (14)	454 (13)	322 (10)	329 (9.3)
c-$HSCS^-$	ν_1 (*A′*)	SH stretch	2241 (289)	1969 (355)	2241 (289)	1968 (355)	2239 (289)	1968 (355)	1610 (148)	1476 (170)
	ν_2 (*A′*)	HSC bend + CS stretch	968 (185)	986 (196)	942 (156)	891 (159)	962 (176)	978 (187)	955 (260)	972 (256)
	ν_3 (*A′*)	HSC bend + CS stretch	832 (151)	796 (147)	825 (163)	791 (153)	829 (155)	793 (151)	661 (70)	639 (68)
	ν_4 (*A′*)	(H)SC stretch	513 (47)	482 (49)	503 (45)	473 (47)	506 (46)	475 (49)	507 (35)	477 (34)
	ν_5 (*A′*)	SCS bend	284 (13)	276 (16)	281 (12)	274 (15)	279 (12)	272 (15)	262 (10)	257 (12)
	ν_6 (*A″*)	SH torsion	528 (0.0)	500 (0.1)	525 (0.0)	497 (0.1)	527 (0.0)	499 (0.1)	417 (0.4)	402 (0.4)

[a] Infrared intensities (in km mol^{-1}) are shown in parentheses.

Table S10 Vibrational wavenumbers (in cm^{-1}) and IR intensities of $HC(S)SH^-$ and its ^{13}C-, ^{34}S- and D-isotopic variants calculated with the B3LYP/aug-cc-pVTZ method

		$HC(S)SH^-$		$H^{13}C(S)SH^-$		$HC(^{34}S)^{34}SH^-$		$DC(S)SH^-$	
Mode	Description	Harmonic	Anharmonic	Harmonic	Anharmonic	Harmonic	Anharmonic	Harmonic	Anharmonic
ν_1	CH stretch	3103 (36)[a]	2950 (53)[a]	3094 (36)[a]	2942 (54)[a]	3103 (36)[a]	2951 (53)[a]	2283 (15)[a]	2203 (22)[a]
ν_2	SH stretch	2384 (445)	2144 (540)	2384 (445)	2144 (540)	2382 (445)	2142 (539)	1713 (226)	1594 (252)
ν_3	HCS deform	1211 (33)	1188 (21)	1208 (30)	1182 (22)	1211 (33)	1186 (25)	821 (10)	807 (11)
ν_4	C═S stretch	912 (56)	888 (63)	888 (35)	865 (52)	905 (52)	882 (60)	960 (89)	941 (76)
ν_5	CSH deform	873 (60)	841 (61)	867 (81)	837 (72)	872 (61)	841 (61)	679 (21)	661 (19)
ν_6	C–S stretch	632 (9.0)	644 (14)	618 (7.9)	636 (13)	626 (9.1)	642 (14)	589 (15)	593 (13)
ν_7	oop CH bend	391 (42)	323 (22)	387 (41)	323 (22)	390 (43)	324 (23)	323 (16)	287 (4.5)
ν_8	SCS bend	288 (8.7)	278 (7.1)	286 (8.7)	277 (6.8)	282 (8.1)	273 (6.1)	271 (13)	258 (17)
ν_9	SH torsion	184 (3.9)	41 (2.9)	183 (3.8)	39 (2.8)	183 (3.8)	41 (2.9)	139 (3.2)	75 (3.1)

[a] Infrared intensities (in km mol^{-1}) are shown in parentheses.

Table S11 Vibrational wavenumbers (in cm^{-1}) and IR intensities of HSCSH calculated with the B3LYP/aug-cc-pVTZ method

Mode (sym.)	Description	Harmonic	Anharmonic
ν_1 (A_1)	in-phase SH stretch	2353 (152)[a]	2145 (165)[a]
ν_2 (A_1)	in-phase in-plane SH bend	986 (28)	944 (24)
ν_3 (A_1)	sym SCS stretch	637 (14)	617 (14)
ν_4 (A_1)	SCS bend	285 (0.2)	265 (0.4)
ν_5 (A_2)	out-of-phase out-of-plane SH bend	591 (0.0)	550 (0.0)
ν_6 (B_1)	in-phase out-of-plane SH bend	535 (3.2)	506 (3.0)
ν_7 (B_2)	in-phase out-of-plane SH stretch	2366 (23)	2160 (29)
ν_8 (B_2)	SCS asym stretch	1052 (102)	1020 (91)
ν_9 (B_2)	out-of-phase in-plane SH bend	931 (7.5)	884 (9.2)

[a] Infrared intensities (in km mol^{-1}) are shown in parentheses.

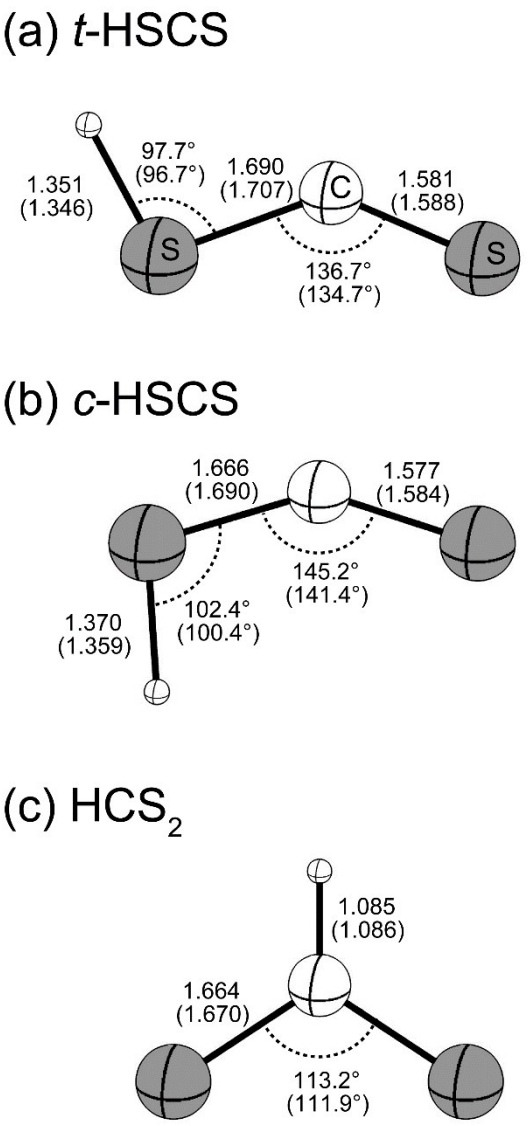

Fig. S1 Geometries of (a) *t*-HSCS, (b) *c*-HSCS, and (c) HCS_2 optimized with the B3LYP/aug-cc-pVTZ method. Geometric parameters obtained with the CCSD(T)/aug-cc-pVTZ method are shown in parentheses for comparison. Bond lengths are in Å.

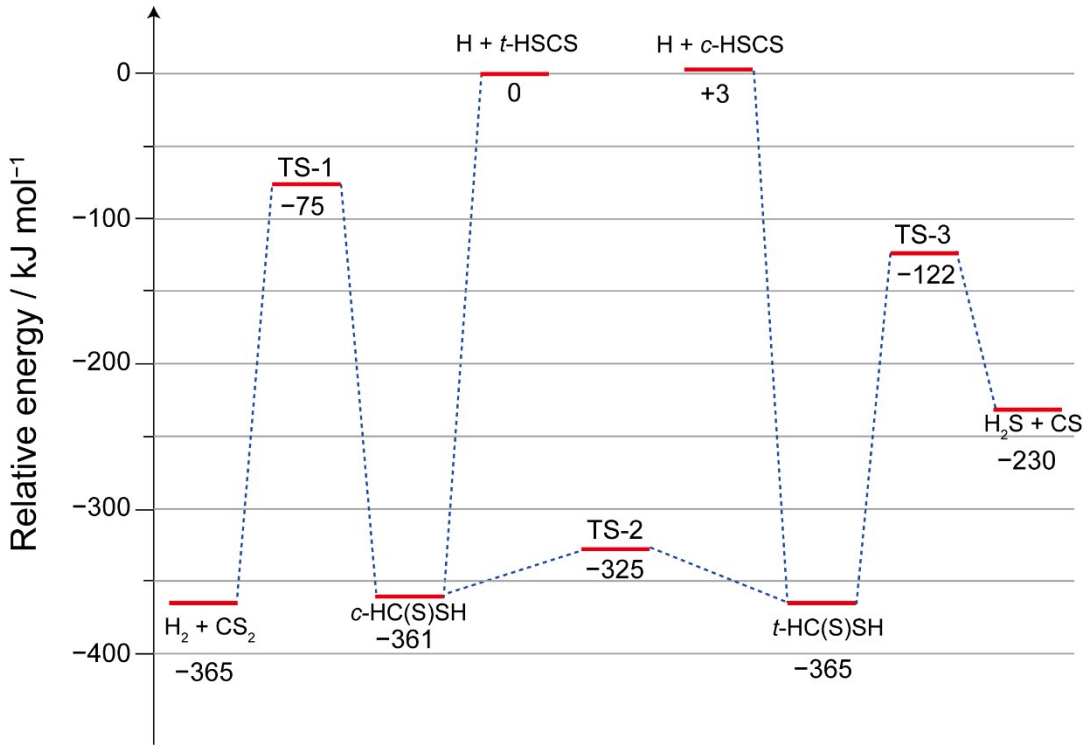

Fig. S2 Potential-energy diagram of the reactions H + *t*-HSCS and H + *c*-HSCS calculated with the CCSD(T)/aug-cc-pVTZ method. The ZPVEs were corrected using harmonic wavenumbers predicted with the same method.

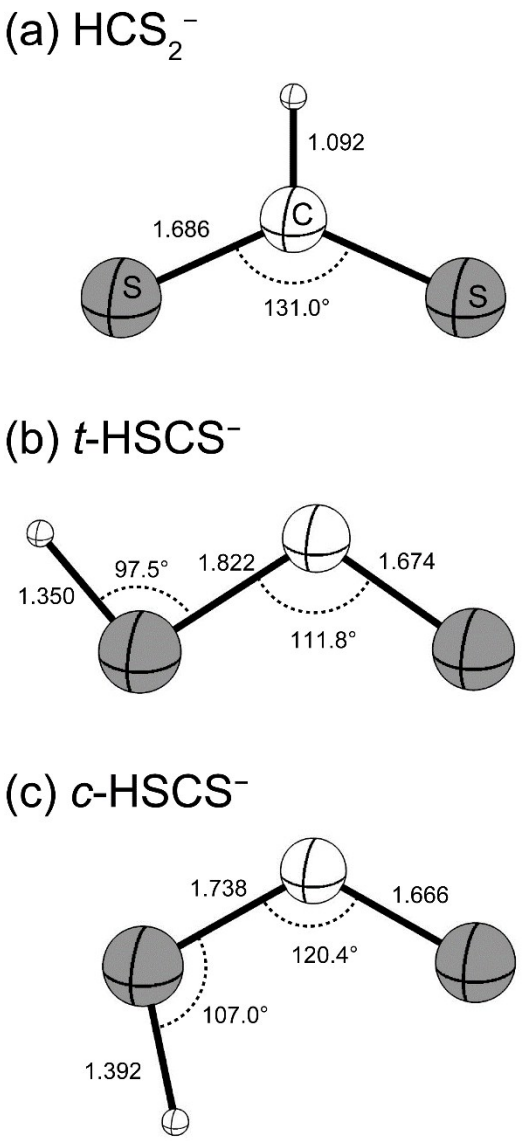

Fig. S3 Geometries of (a) HCS_2^-, (b) *t*-$HSCS^-$, and (c) *c*-$HSCS^-$ optimized with the B3LYP/aug-cc-pVTZ method. Bond lengths are in Å.

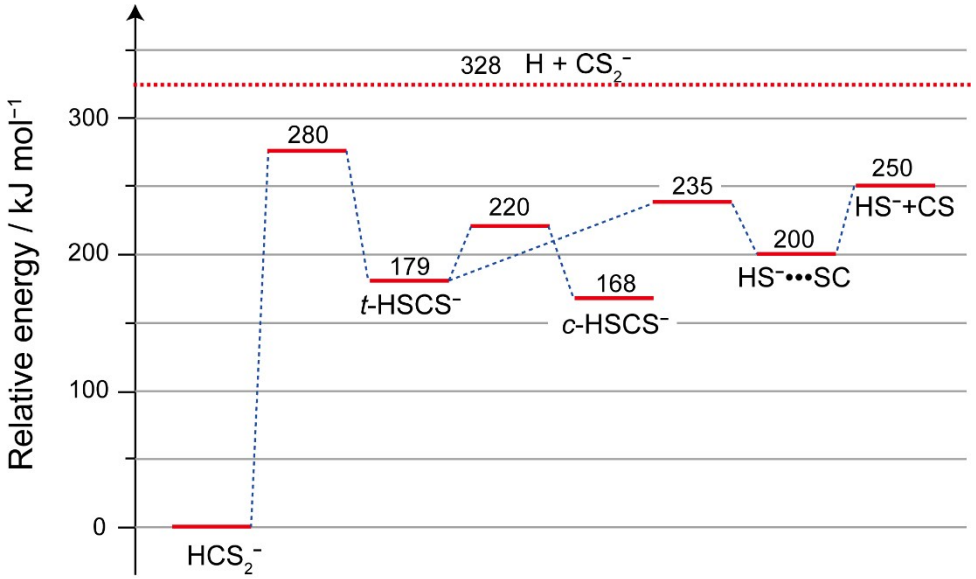

Fig. S4 Potential-energy diagram of the reaction H + CS_2^- calculated with the B3LYP/aug-cc-pVTZ method. The ZPVEs were corrected using harmonic wavenumbers predicted with the same method.

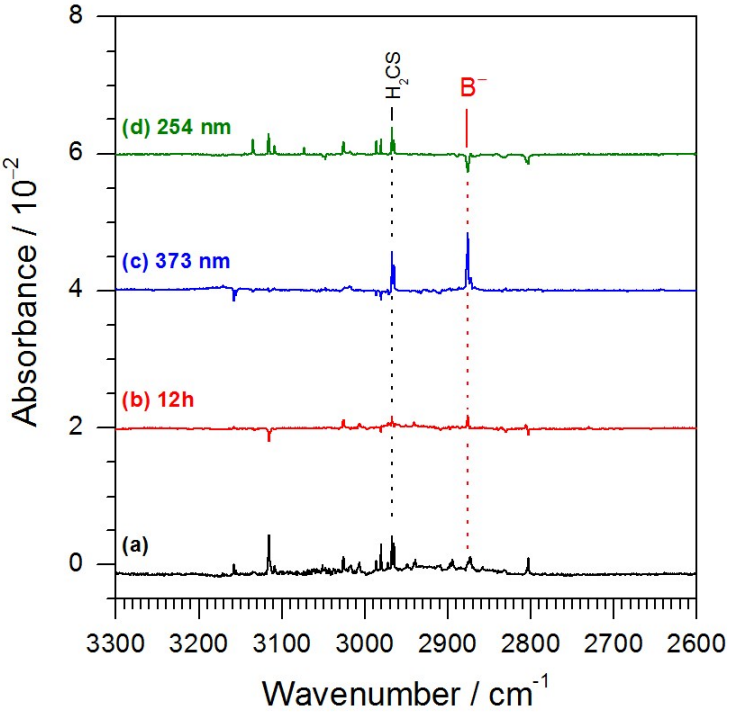

Fig. S5 Partial infrared spectra of experiments with electron bombardment of CS_2/*p*-H_2 in region 3300–2600 cm^{-1}. (a) IR spectrum of a mixture of CS_2/*p*-H_2 (1/2000) bombarded with electrons during deposition at 3.2 K for 7 h; the spectral features of CS_2 were stripped using the IR spectrum of CS_2/*p*-H_2 (1/2000) mixture deposited without electron bombardment. (b) Difference spectrum after maintaining the matrix in darkness for 12 h. (c) Difference spectrum after subsequent irradiation at 373 nm. (d) Difference spectrum after further irradiation at 254 nm. In (b)–(d), lines pointing upward indicate production and those pointing downward indicate destruction in each experimental step. A line at 2875.7 cm^{-1} (marked as B$^-$) is assigned to the CH-stretching (ν_1) mode of HCS_2^- and a line at 2967.0 cm^{-1} is assigned to the CH-stretching (ν_1) mode of H_2CS.

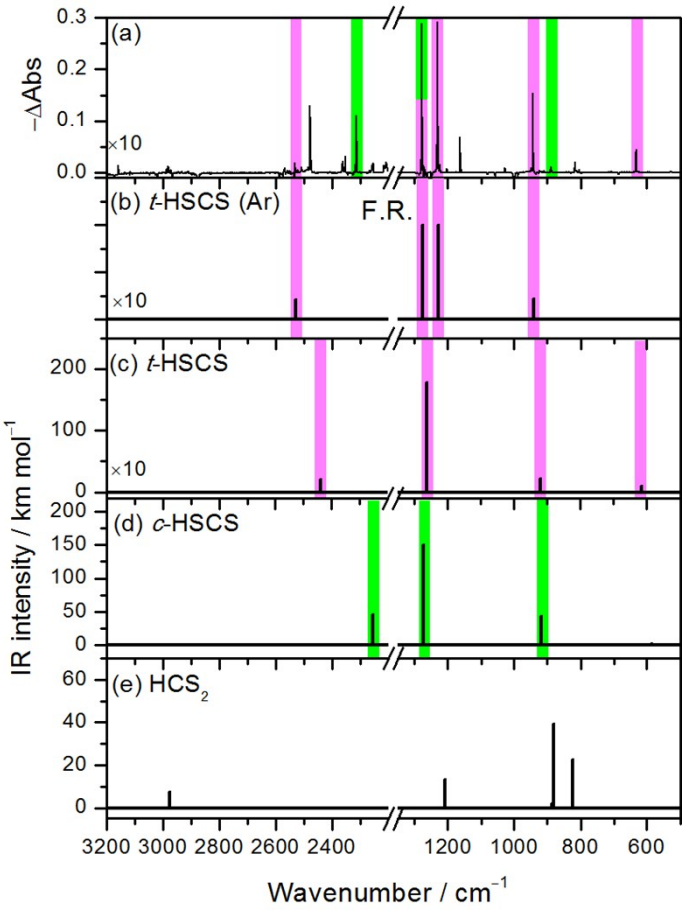

Fig. S6 Comparison of experimental spectrum of an electron-bombarded CS_2/*p*-H_2 matrix with those simulated for possible candidates. (a) Difference spectrum after irradiation at 373 nm; taken from Fig. 3(c) and inverted. Lines at 1278.3, 1231.3, 943.1, and 632.4 cm^{-1} are highlighted by pink color and lines at 2312.7 and 889.0 cm^{-1} are highlighted by green color. (b) Reported spectrum of *t*-HSCS in an Ar matrix, represented with stick spectra; taken from R. B. Bohn, D. Brabson, and L. Andrews, *J. Phys. Chem.*, 1982, **96**, 1582–1589. A pair of lines 1275.2 and 1227.8 cm^{-1} originate from Fermi resonance (marked as F.R.). Simulated stick spectra of (c) *t*-HSCS, (d) *c*-HSCS, and (e) HCS_2 according to anharmonic wavenumbers and IR intensities predicted with the B3LYP/aug-cc-pVTZ method.